Ref.TH.1585-CERN

ANALYSIS OF DATA FOR HYPERCHARGE EXCHANGE REACTIONS

A.C. Irving and A.D. Martin *)
CERN - Geneva

and

V. Barger +)
Physics Department, University of Wisconsin, Madison

A B S T R A C T

The properties of the experimental data on the hypercharge exchange reactions $\pi N \to K\Sigma$, $K\Lambda$ and $\bar{K}N \to \pi\Sigma$, $\pi\Lambda$ in the region 4-16 GeV/c are surveyed, with attention to line reversal inequalities, reaction energy dependences in terms of effective trajectories, phase-energy properties, and SU(3) for exchanges. We determine the s channel helicity non-flip amplitudes at 4 and 14 GeV/c, assuming an exchange degenerate $K_V^* - K_T^*$ Regge pole approximation for the flip amplitudes. In impact parameter only the imaginary parts of the $\pi N \to KY$ non-flip amplitudes (or in terms of exchanges Im K_V^*) are found to be peripheral. All other non-flip amplitude components are central. An SU(3) comparison is made with $K^- p \to \eta\Lambda$, $\eta'\Lambda$ data.

---

*) On leave of absence from the University of Durham, England.

+) John Simon Guggenheim Foundation Memorial Fellow.

Ref.TH.1585-CERN
17 November 1972

I. INTRODUCTION

At present no generally satisfactory global phenomenology exists to account quantitatively for the scattering data on two-body elastic and inelastic reactions [1]. Regge poles, absorption models, and geometrical ideas provide partial and sometimes complementary representations of the data, but a unified over-all picture has not emerged. In these circumstances a worth while first step is to empirically extract, whenever possible, the amplitude components directly from experimental data. These amplitude determinations can then in turn be used to decide among or to formulate theoretical models.

Only in $\pi N \to \pi N$ forward scattering have a sufficient number of observables been measured to carry out an amplitude analysis in a model independent way [2)-5)]. Even this limited amplitude information has had a substantial impact. For example, to reproduce the πN amplitudes, a detailed reformulation of the absorption prescription to include contributions from real parts of rescattering corrections was found to be necessary [6)-10)]. The πN amplitudes supply information only about the P, f, and ρ exchanges and of these the P and f contributions are difficult to disentangle in a unique way [11)]. Consequently only the corrections to the ρ meson Regge pole can be examined directly from rigorous amplitude determinations. The ρ exchange amplitude results suggest the approximate validity of an uncorrected Regge pole form for the s channel helicity flip amplitude F_{+-} [both the zeros and phase are consistent with the pole structure $F_{+-} \sim \alpha(\tan(\pi\alpha/2)+i)$], whereas for the non-flip amplitude the pole form is modified such that $\mathrm{Im}\, F_{++}$ is peripheral (i.e., a "cross-over" zero at $-t \sim 0.2$ GeV^2 and not at $\alpha = 0$).

Ideally, one would like to compare amplitude information on the (ρ, ω, K^*_V) vector exchanges and the (A_2, f, K^*_T) tensor exchanges in pseudoscalar meson-nucleon reactions. All these exchanges have similar particle trajectories $\alpha \simeq 0.5 + t$, with the vector and tensor pole amplitudes 90° out of phase. However, the properties of the exchange amplitudes that can be extracted from the available data are limited. The difference of the $K^\pm p$ cross-sections indicates a cross-over zero in the imaginary part of the ω exchange non-flip amplitude [12)], similar to that found for $\mathrm{Im}\, \rho_{++}$ in πN scattering. A study [1),13)] of $\pi^- p \to \pi^0 n$, ηn, $\eta' n$ and $K^- p \to \bar{K}^0 n$, $K^+ n \to K^0 p$ [and also the set of reactions with the outgoing nucleon replaced by the $\Delta(1236)$] suggests that ρ and A_2 are approximately exchange degenerate in the helicity flip amplitudes *). The behaviour of the $K^\pm p$ elastic

---

*) Recent experiments [14)] in the region of 4 GeV/c indicate that the $K^+ n \to K^0 p$ differential cross-section is larger than that for $K^- p \to \bar{K}^0 n$ by almost a factor of two for $0.3 < -t < 0.6$ GeV^2. If this inequality is confirmed, this implies either that ρ-A_2 exchange degeneracy for the flip amplitude is not valid at 4 GeV/c or that the non-flip contribution is much larger than is currently assumed.

polarizations is further evidence for $\rho - A_2$ exchange degenerate Regge poles in the flip amplitudes.

In addition to the differential cross-section data that are available for the hypercharge exchange reactions $\bar{K}N \to \pi\Sigma, \pi\Lambda$ and $\pi N \to K\Sigma, K\Lambda$, the weak decays of the Λ and Σ^+ yield extensive polarization information. Here the allowed exchanges are the $K_V^*(895)$ and $K_T^*(1420)$ trajectories. Unlike the charge exchange reactions, these processes are not dominated by the flip amplitudes, as evidenced by the sharply forward peaked differential cross-sections. Thus these data should illuminate the non-flip K_V^* and K_T^* exchange amplitudes; in fact, they are probably the best immediately available source of information on tensor exchange amplitudes. If the empirical evidence for unmodified s channel helicity flip Regge pole amplitudes is valid for hypercharge exchange reactions, then an amplitude analysis can be performed from data on an incomplete set of observables. For instance, with plausible assumptions regarding the helicity flip amplitudes, the K_V^* and K_T^* non-flip amplitudes were extracted [15] from the available hypercharge exchange data at 4 GeV/c.

In Section II we collect together all the data for these hypercharge exchange reactions that are available above about 4 GeV/c. For each reaction we summarize the energy dependence in terms of an effective Regge trajectory, $\alpha_{eff}(t)$. In Section III, we update the 4 GeV/c amplitude analysis to include data which have recently become available. Further, we perform an amplitude analysis for the Σ reactions at 14 GeV/c using the effective trajectories to interpolate the cross-sections observed in the different high energy experiments, together with the observed polarization for $\pi^+ p \to K^+ \Sigma^+$. Since the line reversed $(K^- p \to \pi^- \Sigma^+)$ polarization is not measured at high energies we require an additional assumption. From the analysis at 4 GeV/c, we observe that the asymptotic phase-energy relation for non-flip K_T^* exchange is already satisfied, and so it is reasonable to assume that it also holds at 14 GeV/c.

From the resulting amplitudes, we predict the unmeasured observables R and A. We also calculate the $K^- p \to \eta\Lambda$, $\eta'\Lambda$ differential cross-sections and polarizations and compare with the existing data in the region of 4 GeV/c. Finally, the impact parameter representation of the 14 GeV/c amplitudes is discussed.

II. PROPERTIES OF HYPERCHARGE EXCHANGE DATA

Before describing the amplitude determination, we briefly review *) the properties of the experimental data for the reactions $\pi N \to K\Sigma$, $K\Lambda$ and $\bar{K}N \to \pi\Sigma$, $\pi\Lambda$. The available differential cross-section data [17)-21)] above about 4 GeV/c are shown in Figs. 1 and 2. The small angle $\pi^+p \to K^+\Sigma^+$ data of Ref. 17d) below 6 GeV/c are not shown for the sake of clarity. We show $2\sigma(K^-p \to \pi^0\Lambda)$ and $2\sigma(\pi^-p \to K^0\Sigma^0)$ so that these differential cross-sections can be compared directly with those for the other charge states and with those for the line reversed reactions.

A. Shrinkage - Effective Trajectories

The representation of the energy dependences of the differential cross-sections by effective Regge trajectories has often proved to be an illuminating way to study systematics of the data. To determine the effective trajectories from the reaction cross-sections, we use the standard formula

$$\ln\left(\frac{d\sigma}{dt}\right) = \text{constant} + \left[2\alpha_{eff}(t) - 2\right]\ln s$$

at fixed t values. Plots of $\ln(d\sigma/dt)$ versus $\ln s$ at selected t values are shown in Fig. 3 and the effective trajectories are given in Fig. 4. The α_{eff} shown for $\pi p \to K\Sigma$ is based on both $\pi^+p \to K^+\Sigma^+$ and $\pi^-p \to K^0\Sigma^0$ data. However, $\alpha_{eff}(K^+\Sigma^+)$ is considerably higher than $\alpha_{eff}(K^0\Sigma^0)$. This is due to the marked disagreement betwcen the measurements in the two high energy $K\Sigma$ experiments, Refs. 17d) and 18f) (see Fig.3). For $-t \gtrsim 0.2$ all reactions exhibit shrinkage consistent with EXD $K_V^*-K_T^*$ pole behaviour, with the exception of $\bar{K}N \to \pi\Sigma$ which has a flatter effective trajectory. For small $|t|$ the Σ reactions have trajectories which are noticeably higher than those for the Λ reactions.

B. Crossing

The cross-sections for the line reversed pair of reactions $\pi N \to KY$ and $\bar{K}N \to \pi Y$ should be equal asymptotically. However, at momenta in the region of 4-8 GeV/c the cross-sections for the latter reactions are larger by up to a factor of two, with in general the difference decreasing as the forward direction is approached. This is illustrated by the solid curves in Fig. 5 which are

---

*) An earlier review of the salient features of the data may be found in Ref. 16).

obtained by interpolating data in the region of 4 GeV/c, see Fig. 6. At 4 GeV/c such interpolations are based on several experiments for each reaction and, consequently, the problems associated with normalization are reduced. We notice that the inequality of the line reversed cross-sections is larger for the Λ reactions.

At higher energies the situation is not so clear. For instance, the experimental ratio

$$\frac{d\sigma}{dt}(K^- p \to \pi^- \Sigma^+) \Big/ \frac{d\sigma}{dt}(\pi^+ p \to K^+ \Sigma^+)$$

is found to satisfy line reversal equality at 14 GeV/c [17d),19f)], whereas the experiments [18f),19e)] at 16 GeV/c give the same ratio to be about 2 *). The dashed curves in Fig. 5 show the cross-section comparison at 14 GeV/c based on interpolations of all data using the effective trajectory determinations.

C. SU(3) Properties

In Fig. 7, we see that the structures of the polarizations are pairwise similar for $(\pi p \to K\Lambda,\ \pi p \to K\Sigma)$, and also for $(\bar{K}p \to \pi\Lambda,\ \bar{K}p \to \pi\Sigma)$. A plausible qualitative explanation [16),22)] is that the K^* exchange amplitudes in Λ and Σ reactions are related by SU(3) octet symmetry, with the same f/d ratio for the vector and tensor exchanges (but different for helicity flip and non-flip amplitudes). This would be expected if input exchange degenerate K^* poles are corrected in a linear absorption model with comparable final state interactions for $(K\Lambda, K\Sigma)$ and for $(\pi\Lambda, \pi\Sigma)$. A consequence of the SU(3) assumption is that the Σ^0/Λ production ratio at $t = 0$ should be unchanged by line reversal **) and moreover be independent of energy [22)]. The average value of this experimental ratio in the region 4–16 GeV/c is about 0.75 corresponding to a non-flip f (= F/F+D) ratio of $f_+ \approx 1.5$ at $t = 0$. However, there is a tendency for this ratio to increase with energy. This could be due to s channel resonance effects ($\lesssim$ 4 GeV/c) or may simply indicate that the above assumption of identical Λ and Σ final state interactions is not valid.

The corresponding ratio for the spin flip amplitudes, f_-, can be estimated using the polarization relations [22)] :

---

*) Here we use the $\pi^- p \to K^0 \Sigma^0$ data and assume no $I = \frac{3}{2}$ exchange.

**) The data are consistent with the equality

$$\sigma(K^0\Sigma^0)/\sigma(K^0\Lambda) = \sigma(\pi^-\Sigma^+)/4\sigma(\pi^0\Lambda)$$

at $t = 0$.

$$\frac{P\frac{d\sigma}{dt}(K^0\Sigma^0)}{P\frac{d\sigma}{dt}(K^0\Lambda)} = \frac{\frac{1}{4}P\frac{d\sigma}{dt}(\pi^-\Sigma^+)}{P\frac{d\sigma}{dt}(\pi^0\Lambda)} = \frac{3(2f_+-1)(2f_--1)}{(2f_++1)(2f_-+1)}. \qquad (1)$$

The SU(3) assumption is expected to be more reliable for flip amplitudes, than for non-flip amplitudes. However, although Eq. (1) contains both, the estimate of f_- is not particularly sensitive to the input value of f_+, for $f_+ \sim 1.5$. Even so, the data at 4 and 5 GeV/c do not allow an accurate determination of f_-. They suggest that f_- varies with t, decreasing from a value $f_- \sim 0.3$ at $t=0$ to $f_- \sim 0.2$ at $-t = 1$ GeV^2.

III. DETERMINATION OF AMPLITUDES FOR HYPERCHARGE EXCHANGE PROCESSES

In terms of s channel helicity amplitudes ($T_{++} \equiv N$ and $T_{+-} \equiv F$) a complete set of experimental observables for spin 0 – spin $\frac{1}{2}$ scattering is

$$\frac{d\sigma}{dt} = |N|^2 + |F|^2 \qquad (2)$$

$$P\frac{d\sigma}{dt} = 2\,\mathrm{Im}\,(NF^*) \qquad (3)$$

$$R\frac{d\sigma}{dt} = 2\mathrm{Re}(NF^*)\sin\theta_T - (|N|^2-|F|^2)\cos\theta_T \qquad (4)$$

$$A\frac{d\sigma}{dt} = (|N|^2-|F|^2)\sin\theta_T + 2\mathrm{Re}(NF^*)\cos\theta_T . \qquad (5)$$

R and A are the Wolfenstein spin correlation parameters ($P^2+R^2+A^2 = 1$) and θ_T is the scattering angle of the target in the rest frame of the produced baryon. At high energies and small t, θ_T ($\approx \theta_{LAB}$) $\approx \pi/2$. Experimentally, R and A are the components of the recoil baryon polarization for scattering from a target polarized in the reaction plane. Given such a set of observables, it is possible to determine N and F up to an over-all t dependent phase. At present only $d\sigma/dt$ and P measurements exist for the hypercharge exchange reactions, although R and A experiments are underway.

In the reactions $\pi N \to KY$ and $\bar{K}N \to \pi Y$, where $Y = \Sigma$ or Λ, only the natural parity exchanges K_V^* $(1^-,3^-,\ldots)$ and K_T^* $(2^+,4^+,\ldots)$ contribute. The dual amplitudes [23] of the exchange degenerate (EXD) K_V^*-K_T^* Regge pole model for these reactions are *)

$$A_- = A(\bar{K}N \to \pi Y) = K_T^* - K_V^* = -\beta(t)\, s^{\alpha(t)}$$
$$A_+ = A(\pi N \to KY) = K_T^* + K_V^* = -\beta(t)\, e^{-i\pi\alpha(t)}\, s^{\alpha(t)} \quad (6)$$

The $\bar{K}N \to \pi Y$ reactions are described by real amplitudes while the line reversed $\pi N \to KY$ reactions have amplitudes with a rotating phase determined by the EXD trajectory. This dual model leads to equal line reversed differential cross-sections and zero polarizations

$$\frac{d\sigma_+}{dt} = \frac{d\sigma_-}{dt}, \qquad P_+ = P_- = 0. \quad (7)$$

However, we have seen that the forward scattering data show, in general, that

$$\frac{d\sigma_-}{dt} > \frac{d\sigma_+}{dt} \quad (8)$$

by up to a factor of two and large polarizations. Substantial corrections to these input Regge poles are clearly necessary. Our basic assumption, motivated by the $\pi^- p \to \pi^0 n$ amplitude results, is that the physical s channel helicity flip amplitudes are essentially pole-like

$$F_-(s,t) = -\varrho_f$$
$$F_+(s,t) = -\varrho_f\, e^{-i\pi\alpha(t)} \quad (9)$$

where $\varrho_f = \beta(t) p_L^{\alpha(t)}$, with the EXD trajectory phase determined from the particle spectrum, $K_V^*(1^-,895)$ and $K_T^*(2^+,1420)$,

$$\alpha(t) = 0.35 + 0.82t. \quad (10)$$

Equation (9) fixes the over-all phase of the helicity amplitudes.

At a given laboratory momentum p_L, the non-flip amplitudes, which are to be determined from the data, are parametrized in the form

---

*) We use units of s and t in $(\mathrm{GeV})^2$, with residues in $\sqrt{\mu b}/\mathrm{GeV}$ throughout.

$$N_- = -\rho_- \exp(i\phi_-)$$
$$N_+ = -\rho_+ \exp(i\phi_+ - i\pi\alpha). \qquad (10)$$

If K_V^* and K_T^* were EXD in non-flip amplitudes, then we would find $\rho_+ = \rho_-$ and $\phi_\pm = 0$. The magnitudes $\rho_\pm(t)$ and phases $\phi_\pm(t)$ can be calculated from observables

$$\frac{d\sigma_\pm}{dt} = |\rho_\pm|^2 + |\rho_f|^2$$
$$P\frac{d\sigma_\pm}{dt} = 2\rho_f \rho_\pm \sin\phi_\pm, \qquad (11)$$

providing we know the modulus, $|\rho_f(t)|$, of the flip amplitudes. The data impose bounds on $|\rho_f(t)|$, which are useful in estimating this modulus. Using Eqs. (11), we see that the inequalities $|\sin\phi_\pm| \leq 1$ may, upon eliminating $\rho_\pm$, be expressed in the form

$$\tfrac{1}{2}\frac{d\sigma_\pm}{dt}\left(1-\sqrt{1-P_\pm^2}\right) \leq |\rho_f|^2 \leq \tfrac{1}{2}\frac{d\sigma_\pm}{dt}\left(1+\sqrt{1-P_\pm^2}\right). \qquad (12)$$

Below we describe, in turn, the determination of the amplitudes at 4 and 14 GeV/c.

A. Non-Flip Amplitudes at 4 GeV/c

For this analysis, we use the interpolations through the differential cross-section and polarization data shown in Figs. 6 and 7, respectively. These interpolations, when inserted into Eq. (12), give the bounds on the magnitude of the flip amplitude, $|\rho_f(t)|$, which are shown in Fig. 8. The bounds are quite restrictive at the larger t values, particularly for the Λ flip amplitude. If we relate the Λ and Σ flip amplitudes by SU(3),

$$\frac{F(K^+\Sigma^+)}{F(K^0\Lambda)} = \frac{F(\pi^-\Sigma^+)}{-\sqrt{2}\,F(\pi^0\Lambda)} = \sqrt{6}\left(\frac{2f_- - 1}{2f_- + 1}\right), \qquad (13)$$

then the bounds indicate that the f/d ratio f_- should decrease with increasing $-t$, as mentioned in Section II.C. The values of ρ_f which we use in the calculation of the non-flip amplitudes are shown in Fig. 8. Fortunately the precise choice of ρ_f is not crucial to the results.

With the above forms for ρ_f and the data interpolations shown in Figs. 6 and 7, we solve Eqs. (11) for $\rho_\pm$ and $\phi_\pm$ and express the results in terms of the definite signature, K_V^* and K_T^*, non-flip contributions

$$\left.\begin{matrix} K_V^* \\ K_T^* \end{matrix}\right\} = -\frac{1}{2}\left[\rho_+ \exp(i\phi_+ - i\pi\alpha) \mp \rho_- \exp(i\phi_-)\right]. \qquad (14)$$

In the following, this notation (K_V^* and K_T^*) is consistently used to refer to the non-flip exchange contributions. There are four solutions corresponding to the phase ambiguities. We select the solution with $\mathrm{Re}\,K_V^*/\mathrm{Im}\,K_V^* > 0$ and $\mathrm{Re}\,K_T^*/\mathrm{Im}\,K_T^* < 0$ at $t = 0$ to be in agreement with the signs of the pole amplitudes, since the absorptive corrections are not expected to give over-all sign changes at $t = 0$. The results for the non-flip contributions at 4 GeV/c are shown in Fig. 9.

We see that the non-flip amplitudes for the Λ and Σ reactions are qualitatively similar (opposite polarizations, $P_\Lambda \approx -P_\Sigma$, result from ρ_f^Σ and ρ_f^Λ being positive and negative, respectively). In each case $\mathrm{Im}\,K_V^*$ has a cross-over zero at $-t \sim 0.15$ and this suggests that the cross-over is a universal feature of the imaginary parts of the non-flip vector (ρ, ω, K_V^*) exchange amplitudes. On the other hand, $\mathrm{Re}\,K_V^*$ is consistent with Regge pole behaviour ($\mathrm{Re}\,K_V^* \sim \alpha \tan \pi\alpha/2$). The non-flip tensor exchange amplitude is seen to dominate the hypercharge exchange reactions for $-t \lesssim 0.4$ (cf., the table in Section IV). There is no cross-over zero in $\mathrm{Im}\,K_T^*$ near $-t = 0.2$ in contradiction with dual absorption model [24] predictions.

It is illuminating to study the phase-energy properties of the amplitudes. At asymptotic energies there is a definite relation between the phase and the energy dependence of an amplitude. If, at fixed t, $A(s,t) \to (s-u)^{\alpha(t)}$ as $s \to \infty$ then $\mathrm{Re}\,A/\mathrm{Im}\,A \sim -\cot \pi\alpha/2$ [$+\tan \pi\alpha/2$] for a crossing symmetric [anti-symmetric] amplitude. If a logarithmic factor is present this is still true in the limit $\log s \to \infty$ and so the phase $\alpha(t)$ may be interpreted as an effective trajectory. Using this phase-energy relation at 4 GeV/c, we calculate the phase $\alpha_T(t)$ of the (crossing symmetric) non-flip K_T^* amplitude. For the Σ reactions, the result is shown in Fig. 10. Since $\alpha_T(t)$ is consistent with the $\alpha_{\mathrm{eff}}(t)$ found for the Σ data (cf., Fig.4) and since non-flip K_T^* exchange is dominant for $-t \lesssim 0.4$, this suggests the phase-energy relation is approximately valid for the Σ reactions at 4 GeV/c. The corresponding relation is not satisfied for the Λ reactions and may reflect the large difference in the 4 GeV/c Λ line reversed cross-sections (see Fig.5).

The amplitude results for K_V^* exchange indicate that there will not be a simple K_V^* phase energy relation at 4 GeV/c. The quantity $\alpha_V = 2/\pi[\cot^{-1} \times (\mathrm{Im}\, K_V^*/\mathrm{Re}\, K_V^*)]$ calculated from the Σ amplitudes is shown in Fig. 10 and is very different from the expected vector trajectory. In the same figure, we compare α_V with that deduced from the Λ amplitudes and with the corresponding quantity for the ρ exchange non-flip amplitude obtained in an analysis of π N scattering [4]. The similarity of these three independent phase determinations of the non-flip vector exchange amplitudes is striking.

Using SU(3) we can predict from the Σ amplitudes the polarizations in $\pi^- p \to \pi^0 n$ and $\pi^- p \to \eta n$ at 4 GeV/c. As expected from the similarity of the ρ and K_V^* exchange amplitudes the calculated polarization for $\pi^- p \to \pi^0 n$ is in approximate agreement with the data. As tensor exchange obeys the phase-energy relation, we predict the $\pi^- p \to \eta n$ polarization to be small (and positive) at 4 GeV/c.

B. Non-Flip Amplitudes at 14 GeV/c

We repeat the above analysis to determine the Σ reaction amplitudes from the data at 14 GeV/c. To reduce the normalization uncertainties in the high energy experiments, we use the Σ cross-sections obtained by the $\alpha_{\mathrm{eff}}(t)$ interpolation (see Fig.5), together with the interpolation of the high energy $\pi^+ p \to K^+ \Sigma^+$ polarization data, shown in Fig. 11. Since the structure of the $K^- p \to \pi^- \Sigma^+$ polarization is not known at 14 GeV/c we cannot, as we did above, solve directly for the non-flip K_V^* and K_T^* amplitudes. Instead we assume that the K_T^* non-flip amplitude satisfies the phase-energy relation,

$$\mathrm{Im}\, K_T^* = -\tan \frac{\pi \alpha_T}{2}\, \mathrm{Re}\, K_T^*,$$

which, as we have seen, appears to be already valid for K_T^* exchange at 4 GeV/c. Given the phase $\alpha_T(t)$ and the magnitude of the flip amplitudes ($|\rho_f| = (4/14)^{\alpha(t)} |\rho_f(4\ \mathrm{GeV/c})|$) we can then calculate the non-flip amplitudes, K_V^* and K_T^*, from the 14 GeV/c data. The results are shown in Fig. 12 for two different choices of the input phase $\alpha_T(t)$. First we take α_T to be the phase found from the 4 GeV/c K_T^* exchange amplitude ($\alpha_T = 0.65 + 1.14t \approx \alpha_{\mathrm{eff}}$) and secondly we input the EXD pole phase ($\alpha_T = 0.35 + 0.82t$). The non-flip amplitudes (particularly those obtained with the first choice of α_T) have similar structure to those obtained for the Σ reactions at 4 GeV/c. For the second choice of α_T the amplitudes are much more like the EXD pole solution, but even so $\mathrm{Im}\, K_V^*$ has a cross-over zero at $-t = 0.2$.

The predictions for the $K^- p \to \pi^- \Sigma^+$ polarization at 14 GeV/c are shown in Fig. 11. The values of the polarization averaged over the angular distributions, -0.24 and -0.04 depending on the input phase α_T, are to be compared with the experimental value at 14.3 GeV/c [19f], $\langle P_\Sigma \rangle = 0.12 \pm 0.25$.

IV. RELATED PROPERTIES OF HYCEX AMPLITUDES

The analysis of Section III was based on the assumption of EXD pole forms for s channel helicity flip amplitudes. If, on the other hand, we had made the assumption of a pole form for the t channel flip amplitudes, then, since only P and $d\sigma/dt$ data are used, we would simply have to re-interpret the calculated K_V^* and K_T^* as t channel non-flip amplitudes. However, the R and A parameters, Eqs. (4) and (5), do not have frame invariant forms. In Fig. 13 we show the predictions of the R and A parameters at 4 GeV/c resulting from the K_V^* and K_T^* s channel non-flip amplitudes of Fig. 9.

An idea of the exchange composition of the differential cross-section can be obtained from the Table. Here we list the individual flip and non-flip K_V^* and K_T^* exchange contributions to the average of the line reversed cross-sections at 4 GeV/c. Again we see the dominance of non-flip K_T^* exchange for $-t \lesssim 0.4$. The smallness of $|K_V^*|^2$ non-flip for $-t \approx 0.25$ is due to the cross-over zero of $\mathrm{Im}\, K_V^*$ and the minimum of $\mathrm{Re}\, K_V^*$ in this region.

From the 4 and 14 GeV/c Σ reaction amplitudes, we can separate the effective trajectories α^V_{eff} and α^T_{eff} of the $|K_V^*|^2$ and $|K_T^*|^2$ contributions. From the Table we anticipate, and indeed find, that $\alpha^T_{eff} \sim \alpha_{eff}$ for $0 < -t < 0.4$ and that $\alpha^V_{eff} \sim \alpha_{eff}$ for $0.4 < -t < 1.0$, where α_{eff} represents the effective trajectory of the sum of the line reversed cross-sections (cf., Fig.4).

A. Comparison with $K^- p \to \eta\Lambda$, $\eta'\Lambda$ Data

With the assumption that the $K^- p \to \pi^0 \Lambda$, $\eta\Lambda$ and $\eta'\Lambda$ exchange amplitudes are related by SU(3) symmetry [25] :

$$
\begin{aligned}
T(K^- p \to \pi^0 \Lambda) &= K_T^* - K_V^* \\
T(K^- p \to \eta \Lambda) &= -\frac{1}{\sqrt{3}}(\cos\theta + 2S_T \sin\theta) K_T^* - \sqrt{3}\cos\theta\, K_V^* \\
T(K^- p \to \eta' \Lambda) &= -\frac{1}{\sqrt{3}}(\sin\theta - 2S_T \cos\theta) K_T^* - \sqrt{3}\sin\theta\, K_V^* \\
T(\pi^- p \to K^0 \Lambda) &= -\sqrt{2}\, K_T^* - \sqrt{2}\, K_V^*
\end{aligned}
\qquad (15)
$$

where θ is the η, η' mixing angle and S_T is the ratio of singlet to octet couplings of η to (πA_2). Using the K_T^*, K_V^* non-flip (and flip) amplitudes from our 4 GeV/c analysis of the Λ reaction data in Section III, we find the best description of the observed $K^- p \to \eta\Lambda$, $\eta'\Lambda$ cross-section data [19b),19d),26)] with $\theta = -11^\circ$ and $S_T = 1.1$. The comparison is shown in Fig. 14, together with that for the polarizations. By inspection of the $\eta\Lambda$ and $\eta'\Lambda$ cross-sections, we would have anticipated (for small η, η' mixing) the dominance of non-flip K_T^* exchange at small t and a minimum in $|K_V^*|$ near $-t = 0.3$.

B. Impact Parameter Distributions

According to the dual absorption model (DAM) [24)], the non-Pomeron exchanges are dual to the leading direct channel resonances. Taking these resonances to be peripheral, $J \approx qR$, the imaginary parts of the exchange amplitudes must likewise be peripheral. The empirical vector meson exchange amplitudes ϱ, ω, K_V^* do in fact have a peripheral t dependent structure

$$
\begin{aligned}
\mathrm{Im}\, N_V &\sim J_0(R\sqrt{-t}), \\
\mathrm{Im}\, F_V &\sim J_1(R\sqrt{-t}),
\end{aligned}
\qquad (16)
$$

with $R \approx 1$ fermi.

In Fig. 15 we show the impact parameter distributions,

$$
T(b) = \frac{1}{\sqrt{\pi}} \int T(t)\, J_0(b\sqrt{-t})\, \sqrt{-t}\, d\sqrt{-t}, \qquad (17)
$$

of the non-flip Σ reaction amplitudes at 14 GeV/c *), together with their decomposition into vector and tensor exchange components. In terms of reaction amplitudes, only the imaginary part of the $\pi N \to K\Sigma$ amplitude exhibits a peripheral structure (an enhancement for $b \sim 1$ fermi), in agreement with the DAM. The imaginary part of the $\bar{K}N \to \pi\Sigma$ amplitude is central in structure and clearly violates the DAM hypothesis which predicts this component to be zero.

Equivalently the central impact parameter distribution of $\mathrm{Im}\, K_T^*$ is contrary to the DAM idea of peripheral non-exotic imaginary parts. Similar conclusions about the non-peripherality of the imaginary part of the tensor exchange amplitude were obtained in a recent study of the f exchange contribution in π N scattering [11].

An analysis of hypercharge exchange data in terms of amplitudes with peripheral imaginary parts has been performed recently [27]. However, $\mathrm{Im}\, K_V^*$ was considerably greater than $\mathrm{Im}\, K_T^*$ in both the flip and non-flip amplitudes and so the description is outside the DAM hypothesis. The description involves the dominance of vector exchange and is thus contrary to a reasonable interpretation of the $K^- p \to \eta\Lambda$, $\eta'\Lambda$ data.

Further, the lack of peripheral structure in the imaginary part of the $\bar{K}N \to \pi\Sigma$ amplitude (see Fig.15) is also inconsistent with the straightforward expectations of the b^2 pole model of Ref. 28), which predicts imaginary parts, if present, to be of peripheral form.

Clearly in the study of amplitude structure of exchanges, the hypercharge exchange reactions provide a very valuable source of information. Accurate experimental polarization and cross-section measurements on line reversed processes at the same energies, with particular attention to cross-section normalizations are crucially needed to more fully explore the empirical structure and energy dependence of amplitudes.

ACKNOWLEDGEMENTS

It is a pleasure to thank Chris Michael for helpful discussions and his interest in this work. We also thank the experimentalists who communicated their data to us. Part of this work was done with S.R.C. support while one of us (A.C.I.) was at the University of Durham.

*) The results at 4 GeV/c are similar to those shown for $\alpha_T = 0.65 + 1.14t$.

$-t(GeV)^2$	$(ReK_V^*)^2$	$(ImK_V^*)^2$	$(ReK_T^*)^2$	$(ImK_T^*)^2$	$\|F_V\|^2$	$\|F_T\|^2$	$d\bar{\sigma}/dt$
0.05	29.2(7)	5.9(1)	129 (32)	232 (57)	2.8(1)	10.0(2)	409
0.1	12.3(5)	1.1(0)	96 (36)	140 (52)	3.2(1)	15.8(6)	269
0.2	0.5(0)	1.6(1)	63 (51)	38 (31)	1.7(1)	18.9(15)	124
0.3	0.0(0)	5.1(9)	30 (51)	7.9(14)	0.4(1)	14.9(26)	58
0.4	0.1(0)	5.8(19)	12.1(40)	1.3(4)	0.0(0)	11.2(36)	31
0.5	0.1(0)	6.7(31)	6.0(28)	0.1(0)	0.1(1)	8.6(39)	22
0.6	0.3(1)	7.5(41)	3.1(17)	0.0(0)	0.4(2)	6.8(38)	18.1
0.8	1.4(8)	9.9(58)	0.3(2)	0.1(0)	1.1(7)	4.2(25)	17.0
1.0	3.9(22)	8.3(48)	0.9(5)	0.1(0)	1.9(11)	2.3(13)	17.4

TABLE : The composition of the average differential cross-section for Σ reactions at 4 GeV/c. The non-flip amplitudes are denoted by K_V^* and K_T^*, and the flip amplitudes by F_V and F_T. $d\bar{\sigma}/dt \equiv \frac{1}{2}[d\sigma(K^+\Sigma^+)/dt + d\sigma(\pi^-\Sigma^+)/dt]$. The contributions to $d\bar{\sigma}/dt$ are in units of $\mu b/GeV^2$, whereas the numbers in brackets show the percentage contribution.

REFERENCES

1) See recent rapporteur reviews :
C. Michael, in Proceedings of the Oxford Conference on High Energy Collisions (1972);
R.J.N. Phillips, in Proceedings of the Amsterdam Conference on Elementary Particles (1972).

2) F. Halzen and C. Michael, Phys.Letters 36B, 367 (1971).

3) G. Ringland and D.P. Roy, Phys.Letters 36B, 443 (1971).

4) V. Barger and R.J.N. Phillips, Phys.Rev. 187, 2210 (1969).

5) V. Barger and F. Halzen, Phys.Rev. D6, 1918 (1972).

6) B.J. Hartley and G. Kane, Phys.Letters 39B, 531 (1972).

7) M. Ross, Phys.Letters 38B, 321 (1972).

8) R.C. Johnson, Phys.Letters 38B, 325 (1972).

9) A. Martin and P.R. Stevens, Phys.Rev. D5, 158 (1972).

10) J. Anderson and K.J.M. Moriarty, Royal Holloway preprint RHCM 71/4 (1972).

11) V. Barger, K. Geer and F. Halzem, Nuclear Phys. - to be published.

12) M. Davier and H. Harari, Phys.Letters 35B, 239 (1971).

13) C.B. Chiu, Nuclear Phys. 30B, 477 (1971).

14) W. Moninger et al., Illinois University preprint COO-1195-212 (1972) ;
R. Blokzijl et al., Nuclear Phys. - to be published.

15) V. Barger and A.D. Martin, Phys.Letters 39B, 379 (1972).

16) A.C. Irving, A.D. Martin and C. Michael, Nuclear Phys. B32, 1 (1971).

17) $\pi^+ p \to K^+ \Sigma^+$:
a) 4.0, 5.05, 7.0 GeV/c : S.M. Pruss et al., Phys.Rev.Letters 23, 189 (1969);
b) 4.0, 5.0 GeV/c : K.S. Han et al., Phys.Rev.Letters 24, 1353 (1970);
c) 5.0, 7.0 GeV/c : P. Kalbaci et al., Phys.Rev.Letters 27, 74 (1971);
d) 6, 10, 14 GeV/c : A. Bashian et al., Phys.Rev. D4, 2667 (1972).

FIGURE CAPTIONS

Figure 1 The high energy differential cross-section data for $K^-p \to \pi^-\Sigma^+$, $\pi^+p \to K^+\Sigma^+$ and $\pi^-p \to K^0\Sigma^0$ from Refs. 19), 17) and 18) respectively. The laboratory momentum is shown in GeV/c.

Figure 2 The high energy differential cross-section data for $K^-p \to \pi^0\Lambda$, $K^-n \to \pi^-\Lambda$ and $\pi^-p \to K^0\Lambda$ from Refs. 19), 20) and 18) respectively. The laboratory momentum is shown in GeV/c. In general $2\sigma(\pi^0\Lambda) > \sigma(\pi^-\Lambda)$ at a given energy, whereas isospin requires equality. The $\bar{K}N \to \pi\Lambda$ data at 6 GeV/c [21] are for $K_L^0p \to \pi^+\Lambda$.

Figure 3 A comparison of the line-reversed cross-section data as a function of $\ell n\, s$ at the fixed t values of -0.1, -0.3 and -0.6 GeV^2. The incident laboratory momentum is shown on the upper axis. In general the $\bar{K}N \to \pi Y$ cross-sections (shown by circles) are larger than those for $\pi N \to KY$ (shown by triangles). The lines correspond to the α_{eff} values shown in Fig. 4.

Figure 4 The effective trajectories, $\alpha_{eff}(t)$, determined from the energy dependence of the reaction cross-section data of Figs. 1 and 2. The EXD K_V^*, K_T^* trajectory, $\alpha = 0.35 + 0.82\ t$, is also shown.

Figure 5 Comparison of the line reversed cross-sections at 4 and 14 GeV/c. The continuous curves are the interpolations of the data around 4 GeV/c of Fig. 6 [here we show $2\sigma(\pi^0\Lambda)$]. The dashed curves are the 14 GeV/c data interpolations obtained using smoothed α_{eff} values from Fig. 4.

Figure 6 Hypercharge exchange cross-section data in the region of 4 GeV/c, together with interpolating curves.

Figure 7 Hypercharge exchange polarization data in the region of 4 GeV/c, together with interpolating curves.

Figure 8 The dashed curves are the bounds [Eq. (12)] on the square of the modulus of the flip amplitude, $|\rho_f|^2$, at 4 GeV/c. The solid curves are the values used in the determination of the non-flip amplitudes. The Λ and Σ curves are related by Eq. (13) with f_- deduced from Eq. (1), using $P\sigma(\Sigma^0)/P\sigma(\Lambda) = -0.43 + 0.22\ t$ and $f_+ = \frac{3}{2}$.

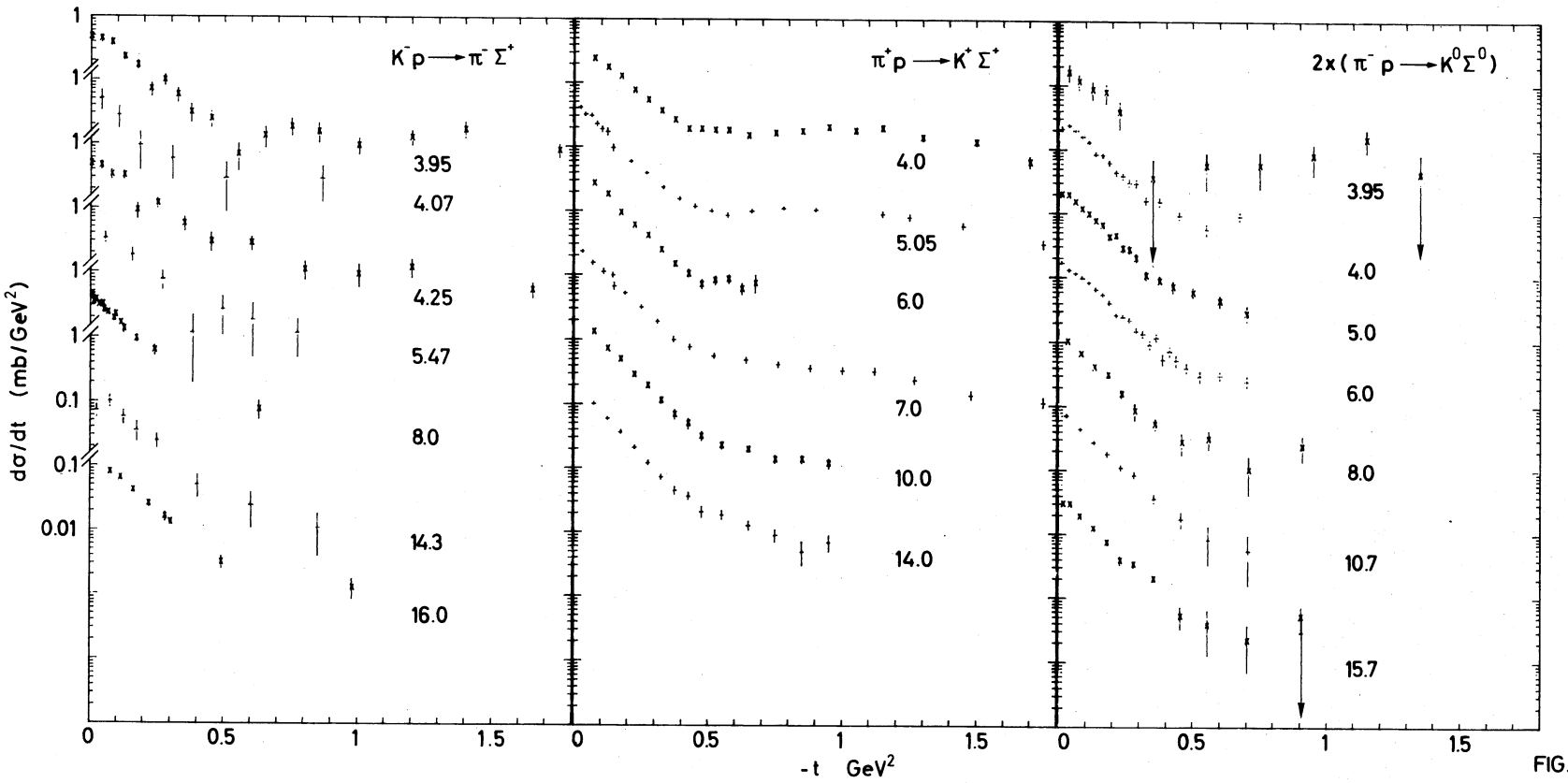
K⁻p → π⁻Σ⁺
π⁺p → K⁺Σ⁺
2x(π⁻p → K⁰Σ⁰)
3.95
4.07
4.25
5.47
8.0
14.3
16.0
4.0
5.05
6.0
7.0
10.0
14.0
3.95
4.0
5.0
6.0
8.0
10.7
15.7
dσ/dt (mb/GeV²)
-t GeV²
0
0.5
1
1.5
0.01
0.1
1

FIG.1

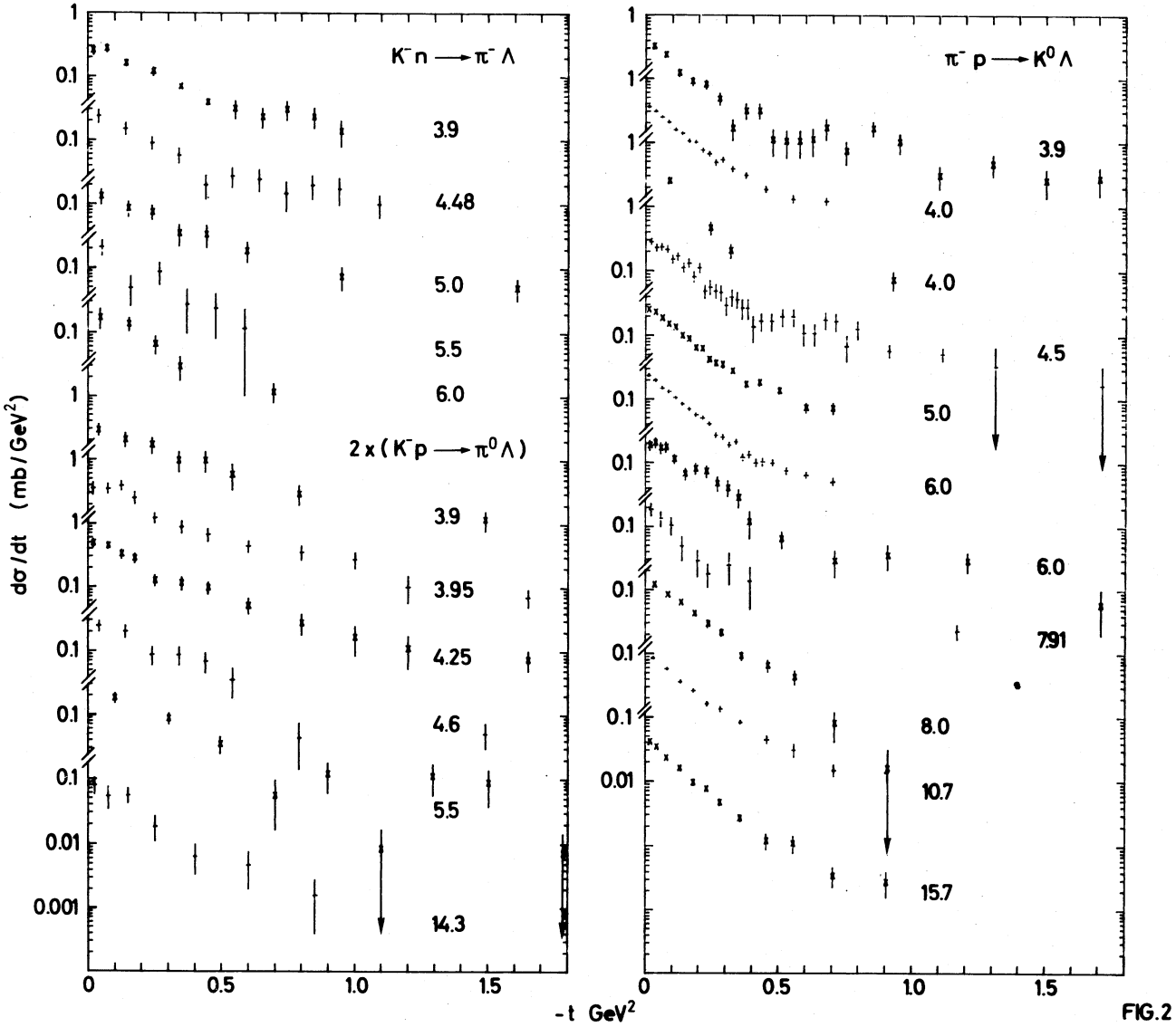
K⁻n → π⁻Λ
3.9
4.48
5.0
5.5
6.0
2 x (K⁻p → π⁰Λ)
3.9
3.95
4.25
4.6
5.5
14.3
π⁻p → K⁰Λ
3.9
4.0
4.0
4.5
5.0
6.0
6.0
7.91
8.0
10.7
15.7
dσ/dt (mb/GeV²)
-t GeV²
0
0.5
1.0
1.5
1
0.1
0.01
0.001

FIG.2

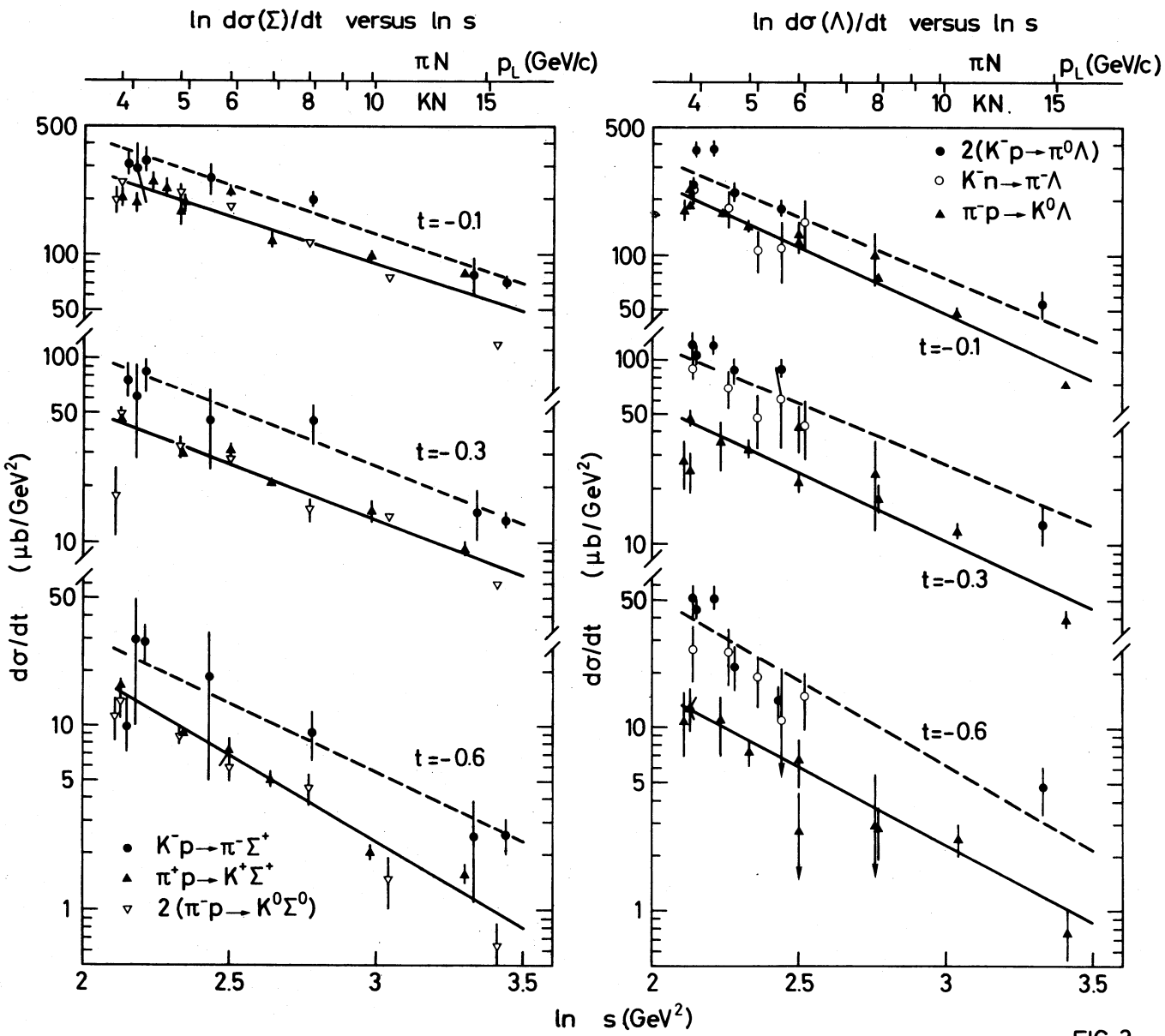
ln dσ(Σ)/dt versus ln s
ln dσ(Λ)/dt versus ln s
πN p_L (GeV/c)
4 5 6 8 10 KN 15
dσ/dt (μb/GeV²)
t=-0.1
t=-0.3
t=-0.6
K⁻p→π⁻Σ⁺
π⁺p→K⁺Σ⁺
2(π⁻p→K⁰Σ⁰)
2(K⁻p→π⁰Λ)
K⁻n→π⁻Λ
π⁻p→K⁰Λ
ln s (GeV²)

FIG. 3

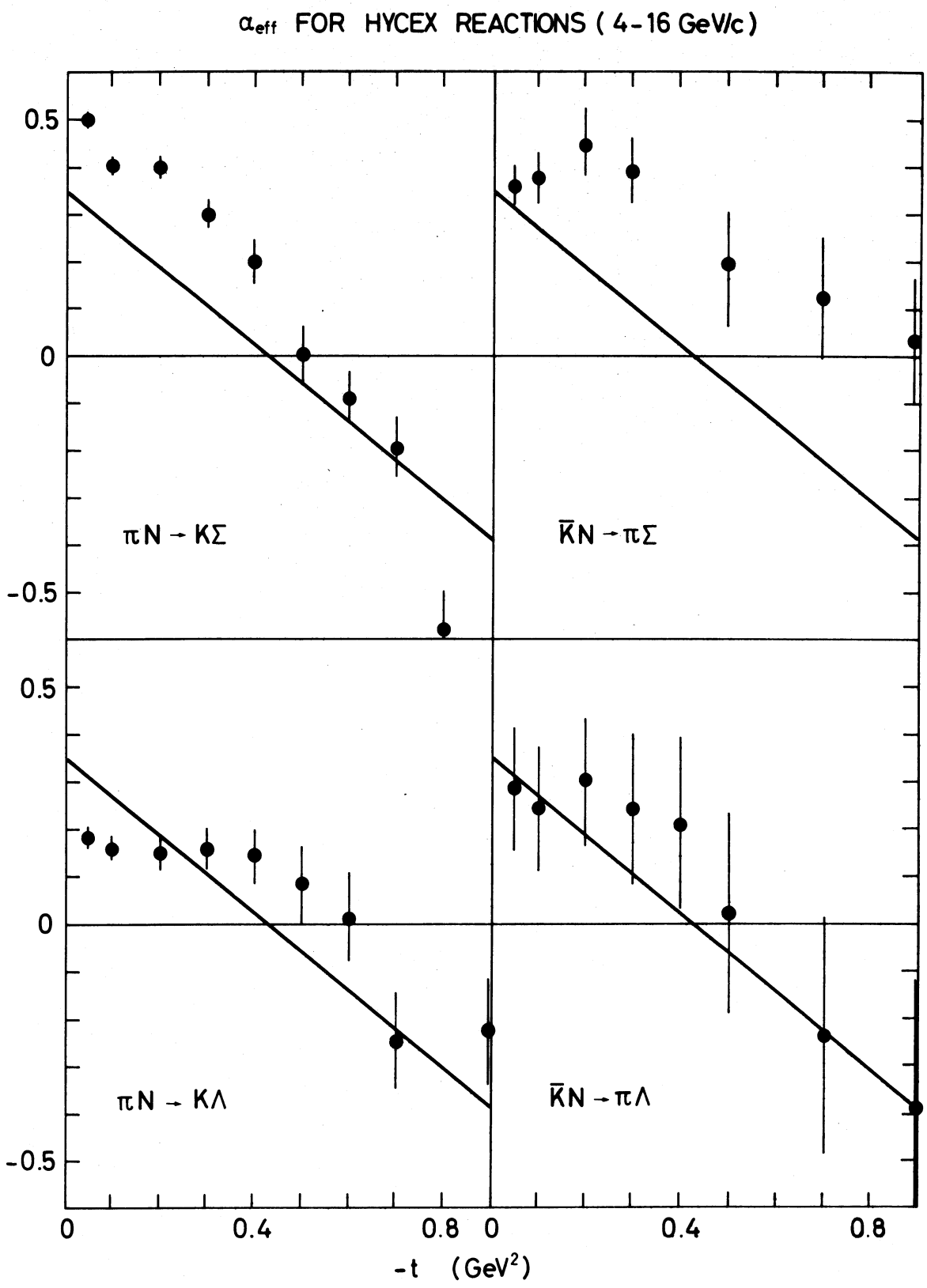
α_{eff} FOR HYCEX REACTIONS (4-16 GeV/c)
0.5
0
-0.5
$\pi N \to K\Sigma$
$\bar{K}N \to \pi\Sigma$
$\pi N \to K\Lambda$
$\bar{K}N \to \pi\Lambda$
0
0.4
0.8
$-t$ (GeV^2)

FIG. 4

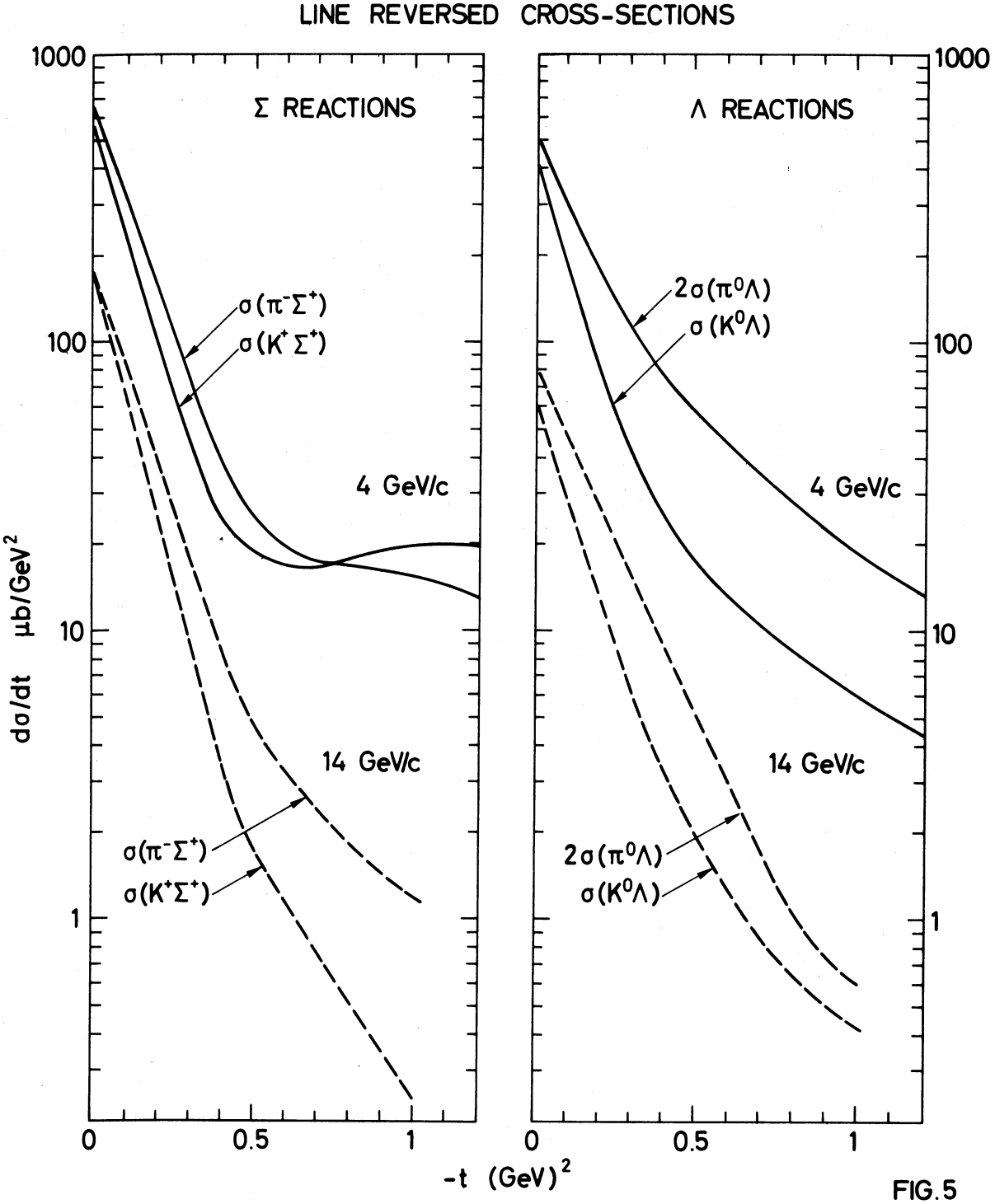
LINE REVERSED CROSS-SECTIONS
Σ REACTIONS
Λ REACTIONS
1000
100
10
1
dσ/dt μb/GeV²
σ(π⁻Σ⁺)
σ(K⁺Σ⁺)
2σ(π⁰Λ)
σ(K⁰Λ)
4 GeV/c
14 GeV/c
0
0.5
1
-t (GeV)²

FIG.5

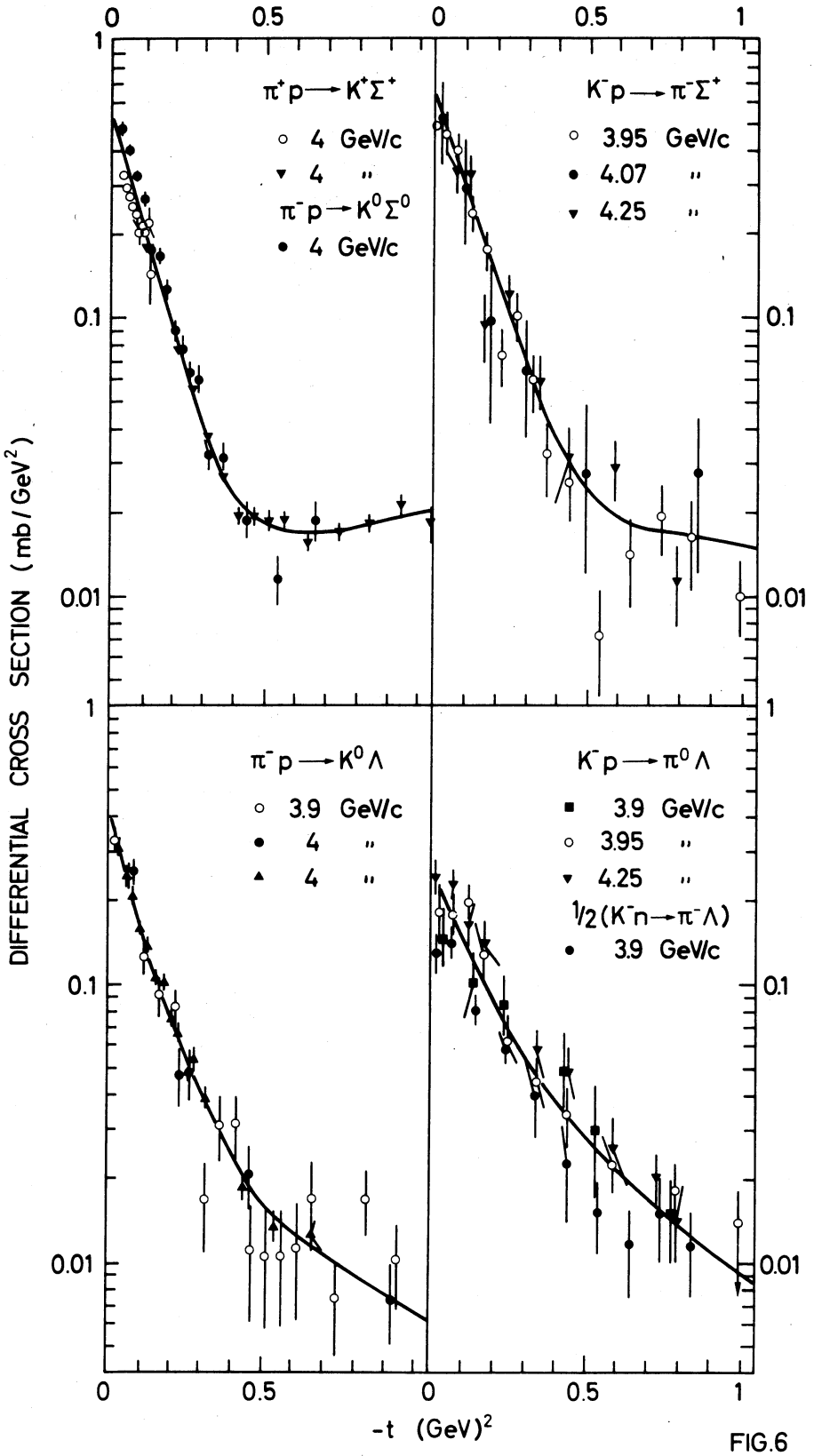
$\pi^+ p \rightarrow K^+ \Sigma^+$
4 GeV/c
4 "
$\pi^- p \rightarrow K^0 \Sigma^0$
4 GeV/c
$K^- p \rightarrow \pi^- \Sigma^+$
3.95 GeV/c
4.07 "
4.25 "
$\pi^- p \rightarrow K^0 \Lambda$
3.9 GeV/c
4 "
4 "
$K^- p \rightarrow \pi^0 \Lambda$
3.9 GeV/c
3.95 "
4.25 "
$\frac{1}{2}(K^- n \rightarrow \pi^- \Lambda)$
3.9 GeV/c
DIFFERENTIAL CROSS SECTION (mb/GeV^2)
-t (GeV)^2
0
0.5
1
0.1
0.01

FIG.6

POLARISATION IN HYCEX REACTIONS

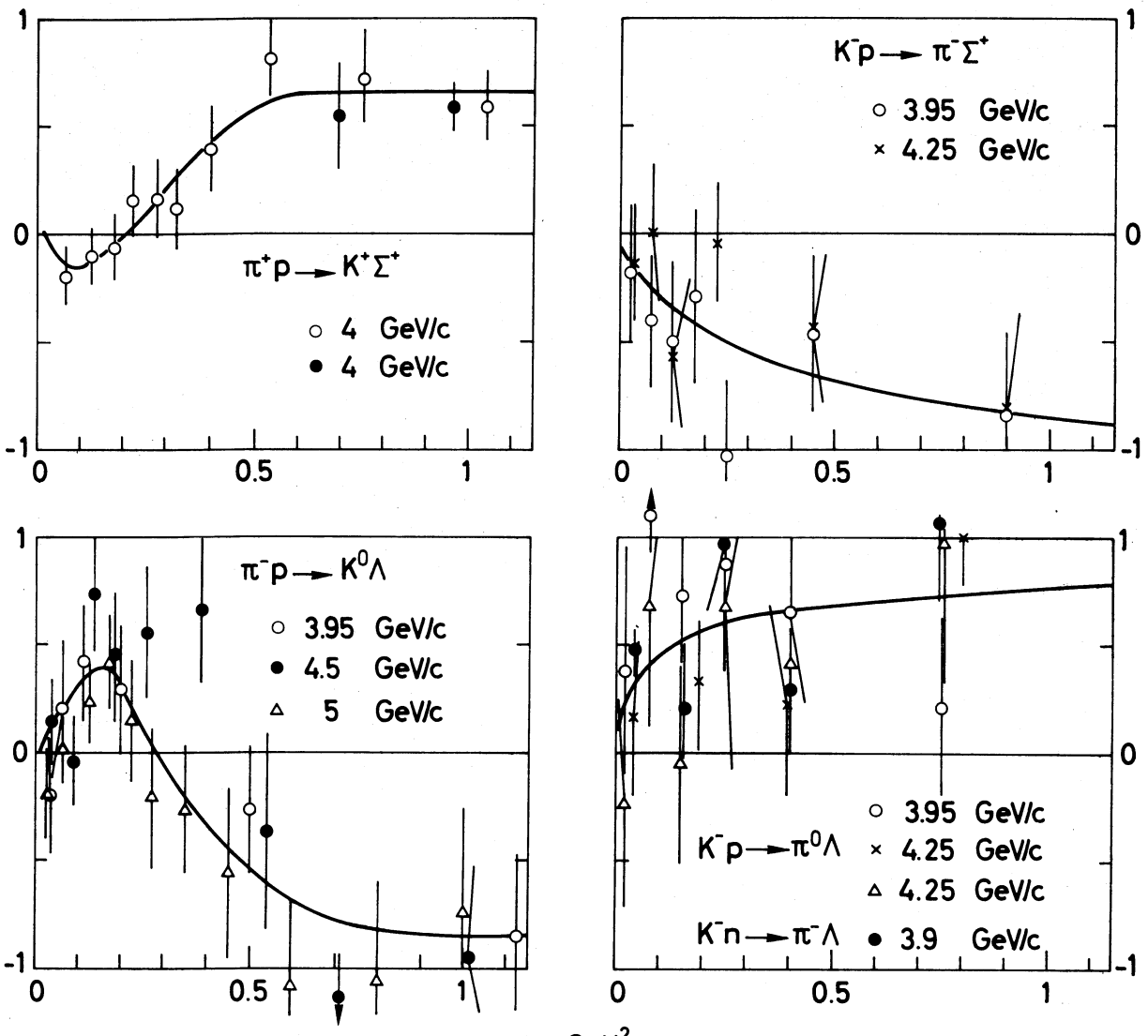

FIG.7

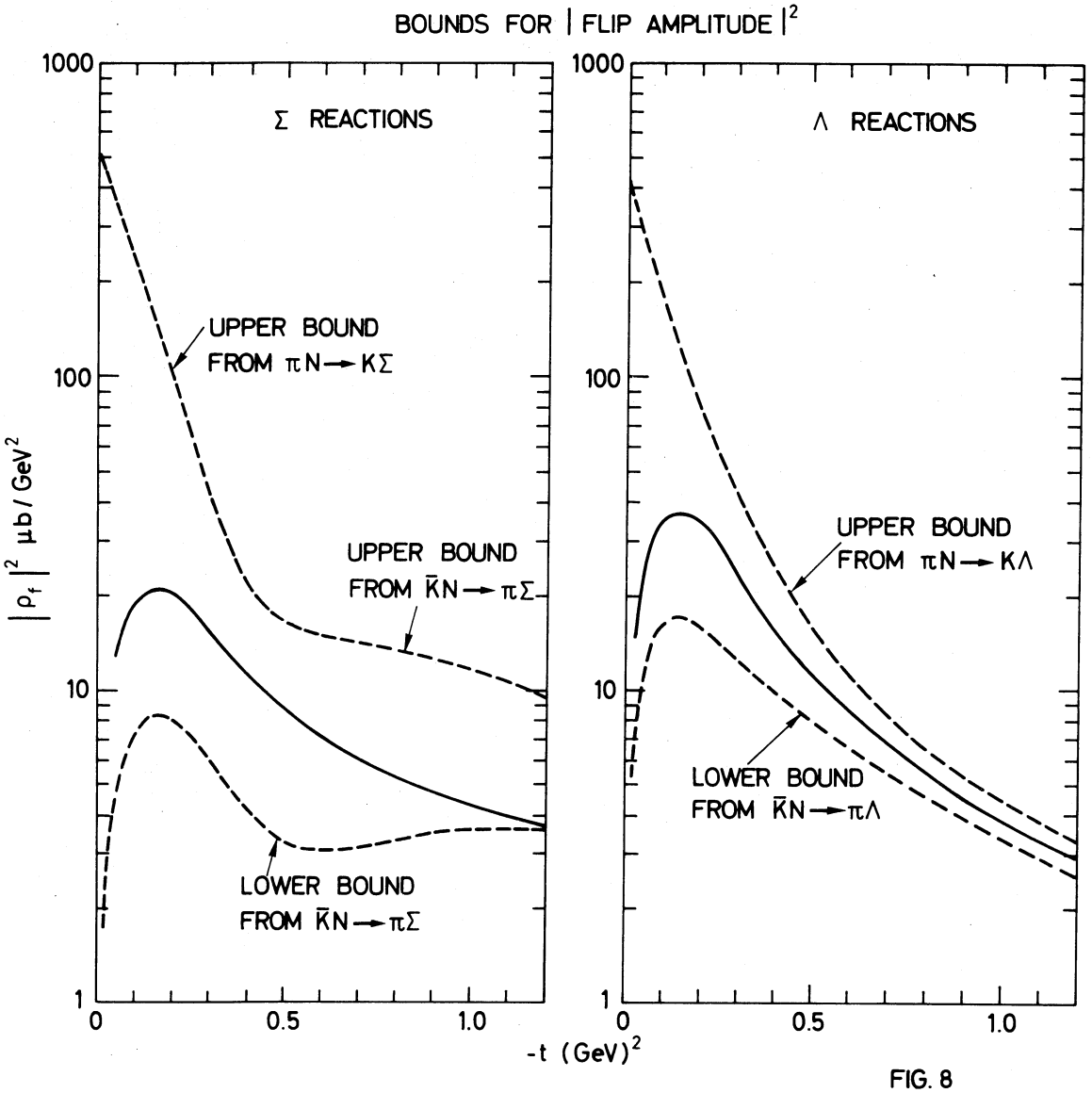
BOUNDS FOR | FLIP AMPLITUDE |²
Σ REACTIONS
Λ REACTIONS
UPPER BOUND
FROM πN → KΣ
UPPER BOUND
FROM K̄N → πΣ
LOWER BOUND
FROM K̄N → πΣ
UPPER BOUND
FROM πN → KΛ
LOWER BOUND
FROM K̄N → πΛ
|ρf|² μb/GeV²
1000
100
10
1
0
0.5
1.0
-t (GeV)²

FIG. 8

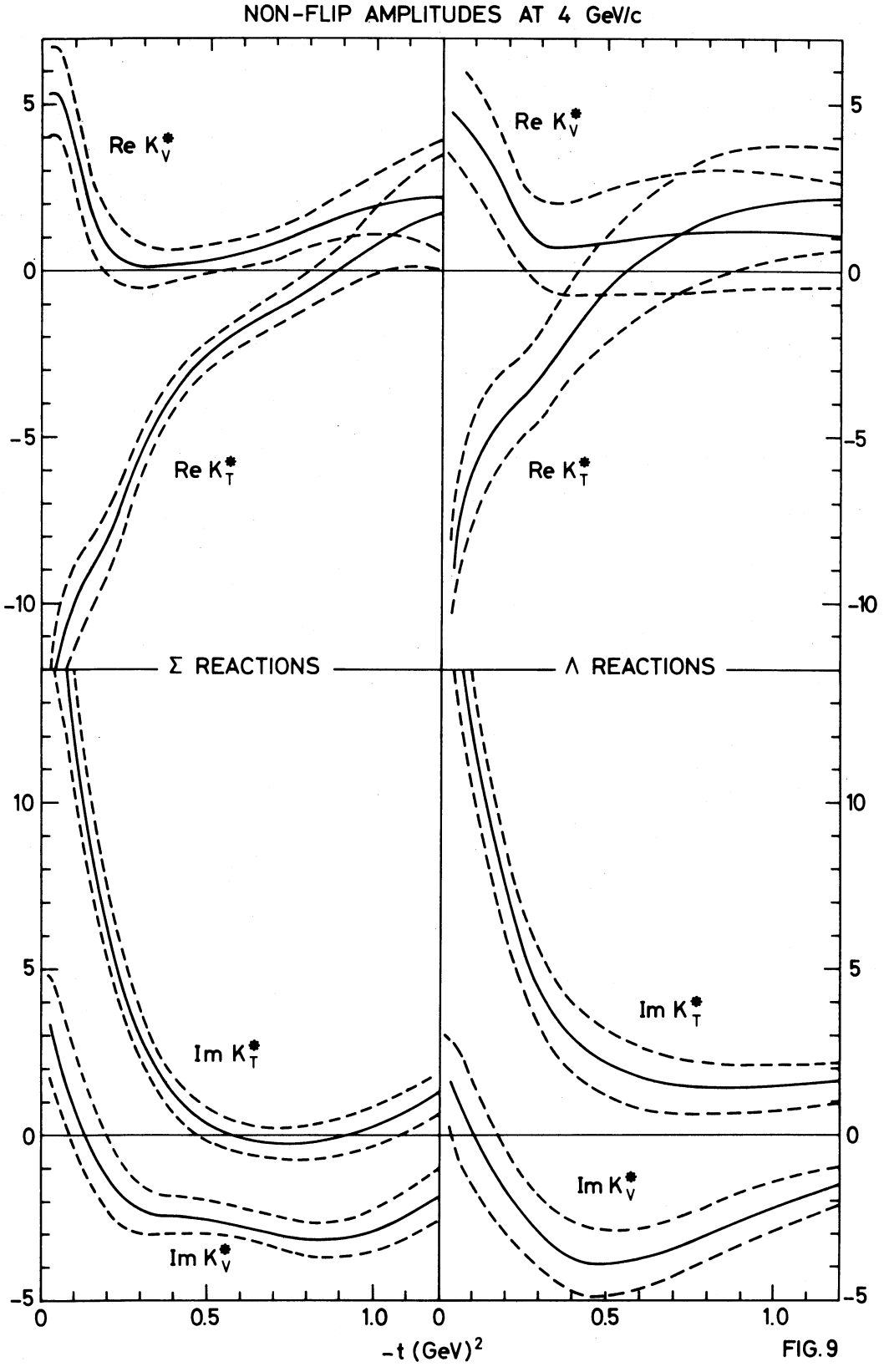
NON-FLIP AMPLITUDES AT 4 GeV/c
Re K*V
Re K*T
Re K*V
Re K*T
Σ REACTIONS
Λ REACTIONS
Im K*T
Im K*V
Im K*T
Im K*V
5
0
-5
-10
10
0.5
1.0
-t (GeV)2

FIG. 9

PHASE PROPERTIES OF NON-FLIP AMPLITUDES IN Σ REACTIONS

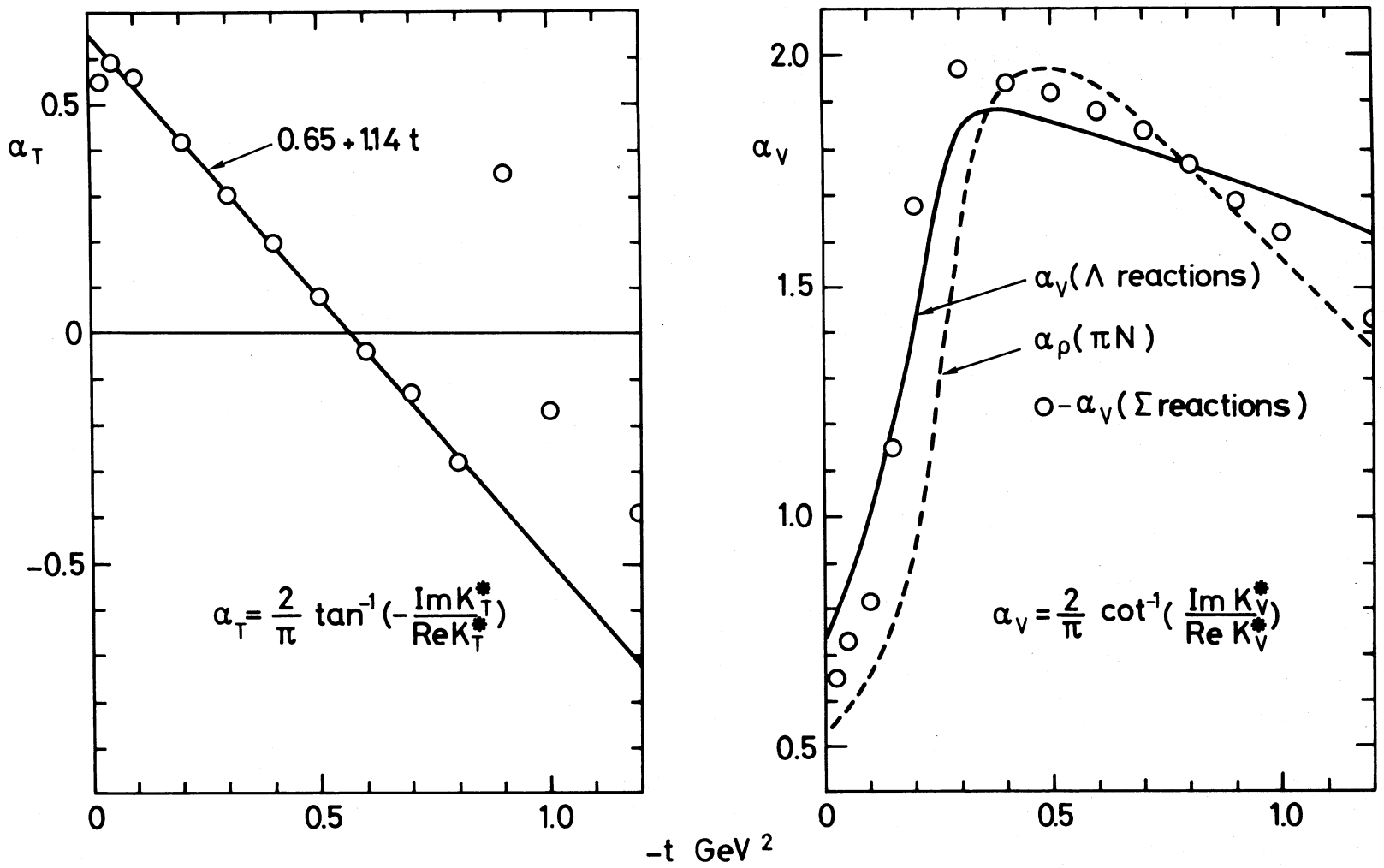

FIG.10

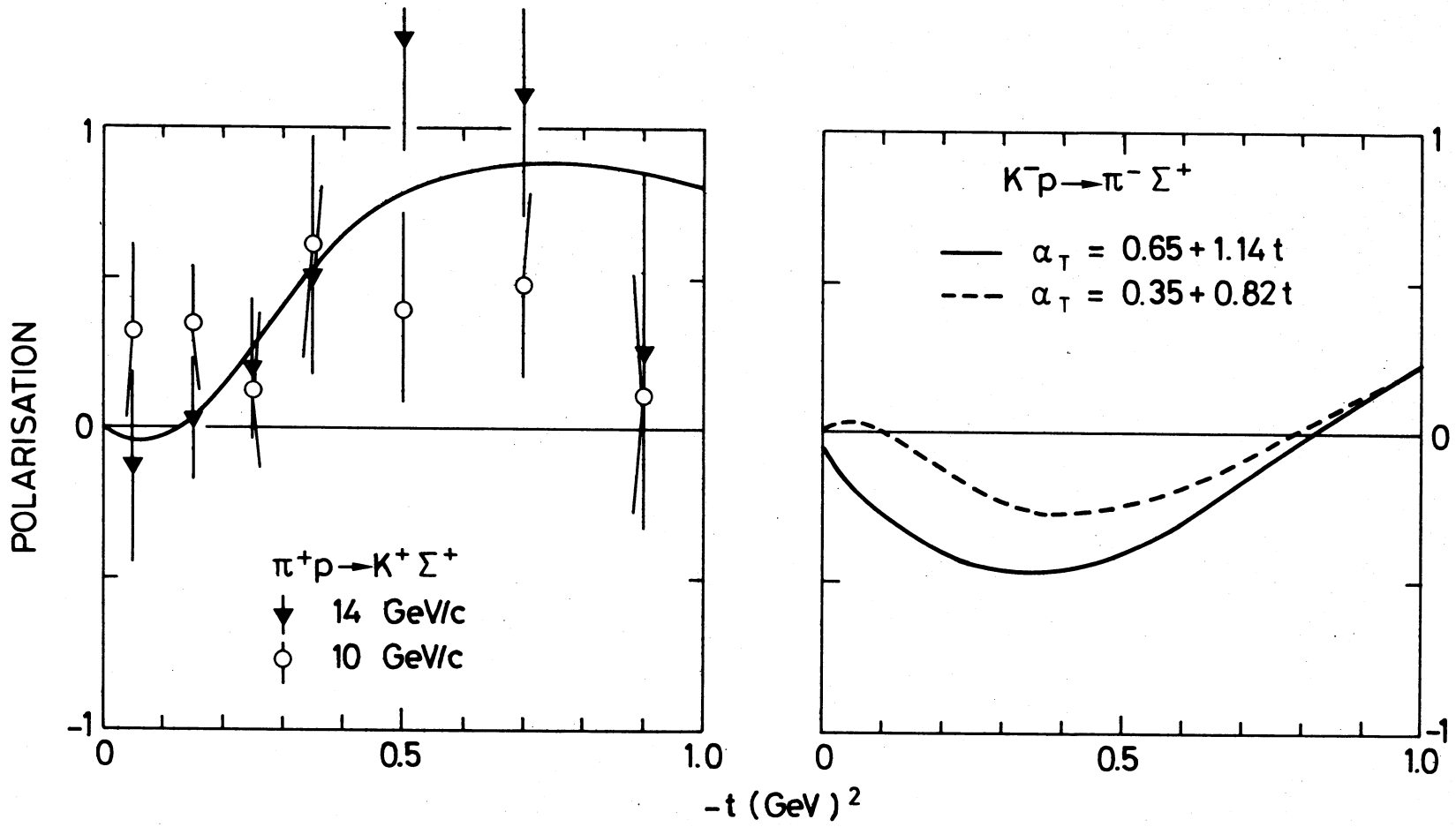

14 GeV/c POLARISATION

FIG 11

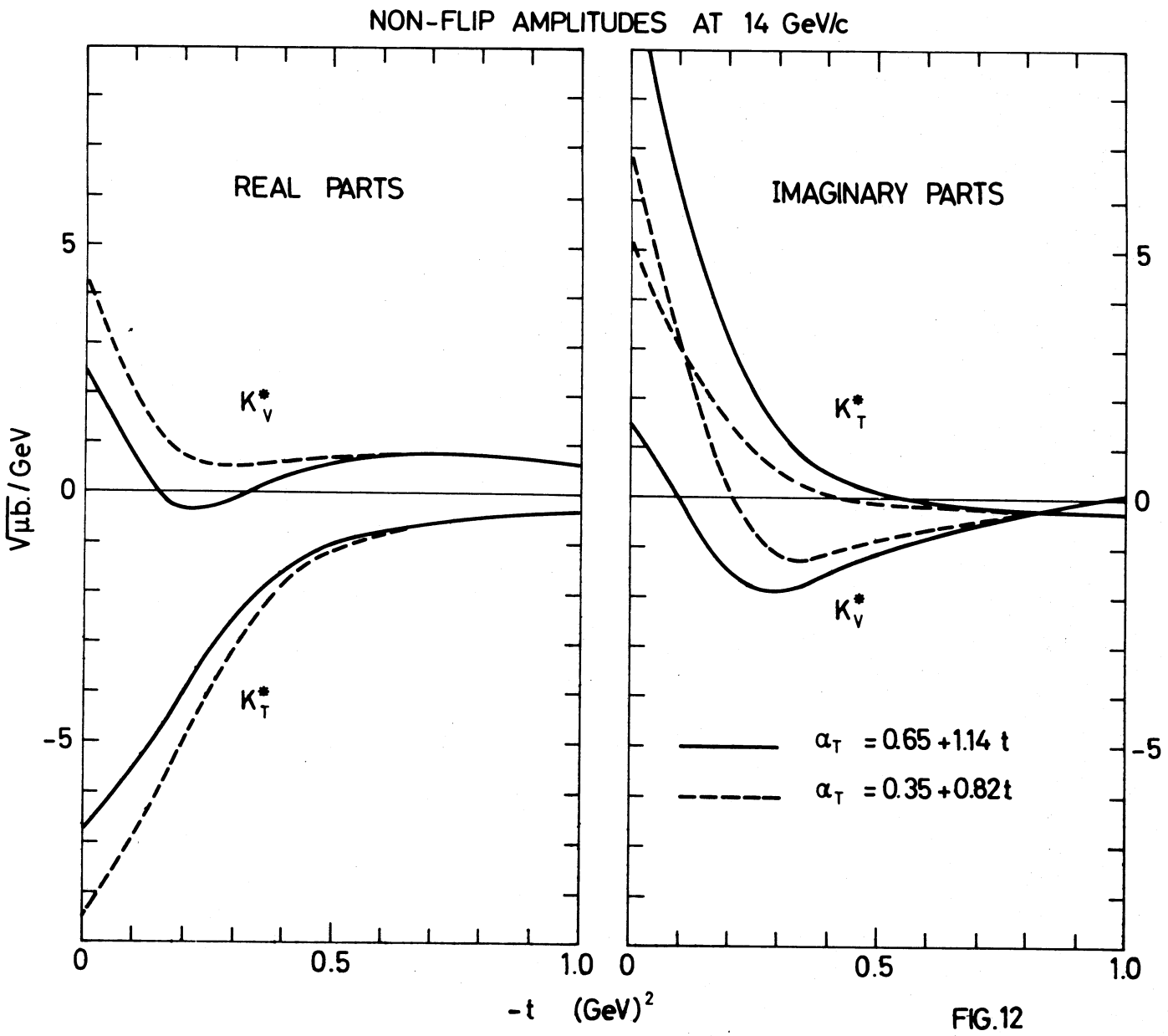
NON-FLIP AMPLITUDES AT 14 GeV/c
REAL PARTS
IMAGINARY PARTS
K^*_V
K^*_T
K^*_T
K^*_V
$\alpha_T = 0.65 + 1.14\ t$
$\alpha_T = 0.35 + 0.82 t$
$\sqrt{\mu b.}$ / GeV
5
0
-5
0
0.5
1.0
$-t$ $(GeV)^2$

FIG.12

IMPACT PARAMETER DISTRIBUTION

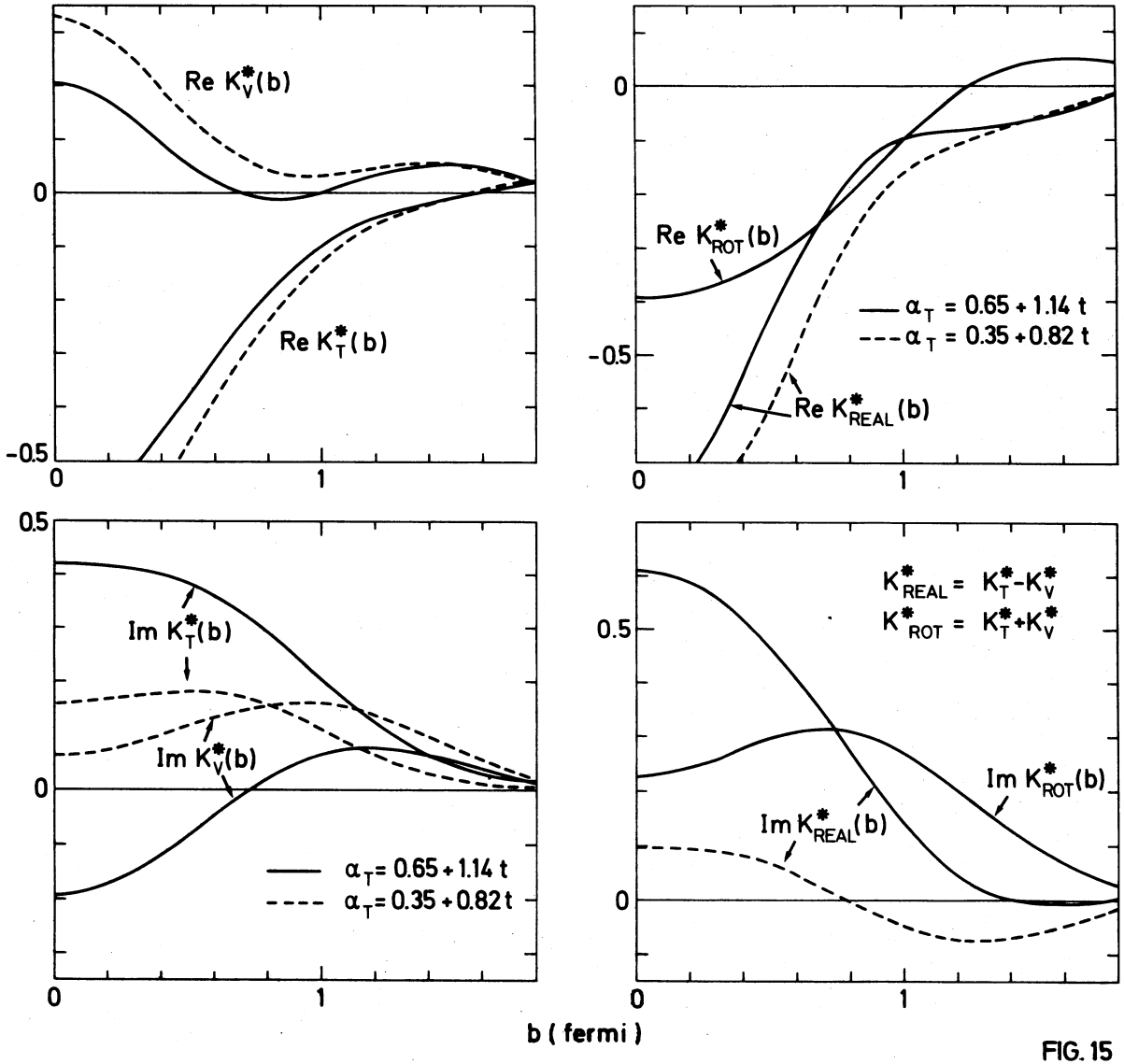

FIG. 15

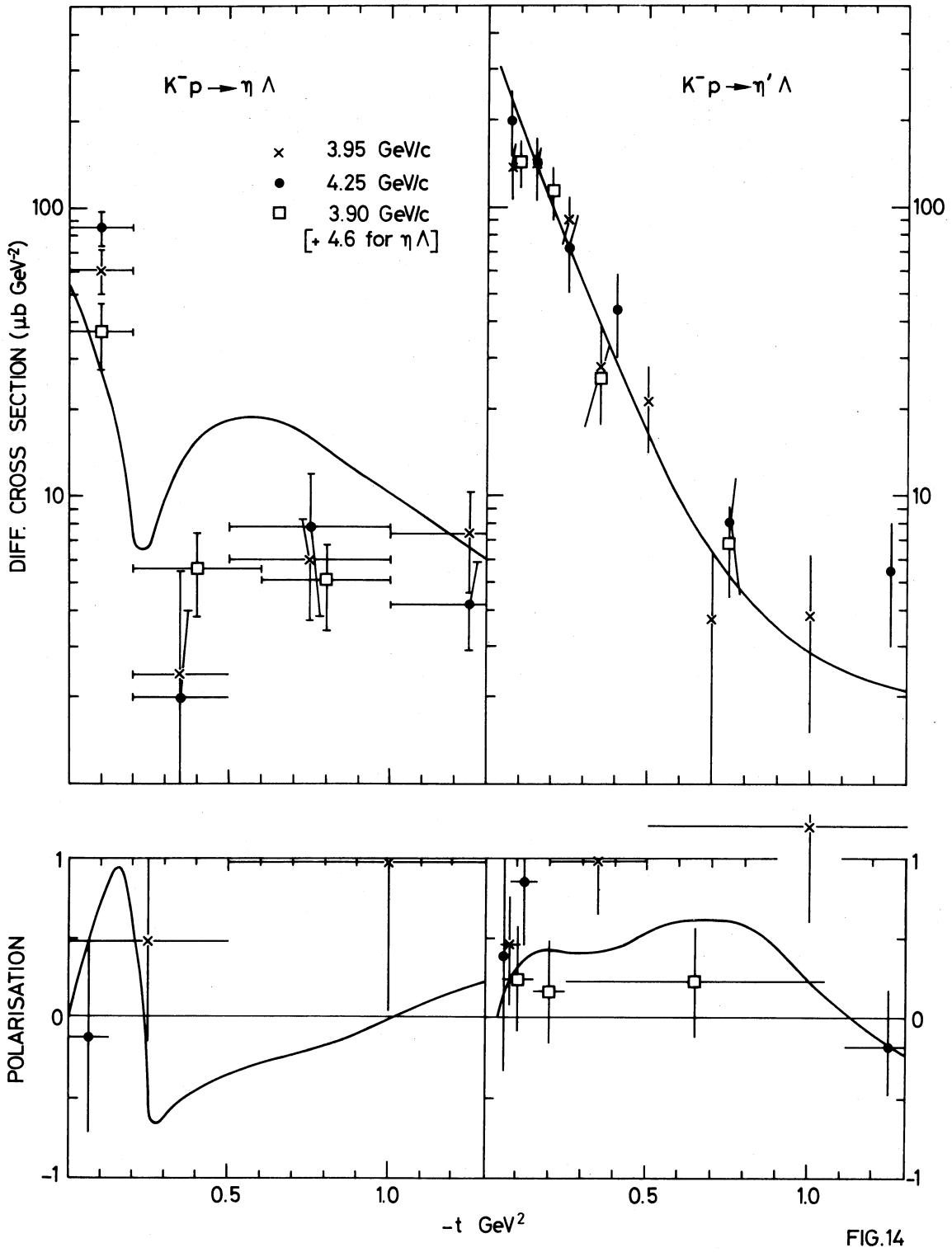
K⁻p → η Λ
K⁻p → η' Λ
× 3.95 GeV/c
• 4.25 GeV/c
□ 3.90 GeV/c
[+ 4.6 for η Λ]
DIFF. CROSS SECTION (μb GeV⁻²)
100
10
POLARISATION
1
0
-1
0.5
1.0
-t GeV²

FIG.14

SPIN CORRELATION PARAMETERS (4 GeV/c)

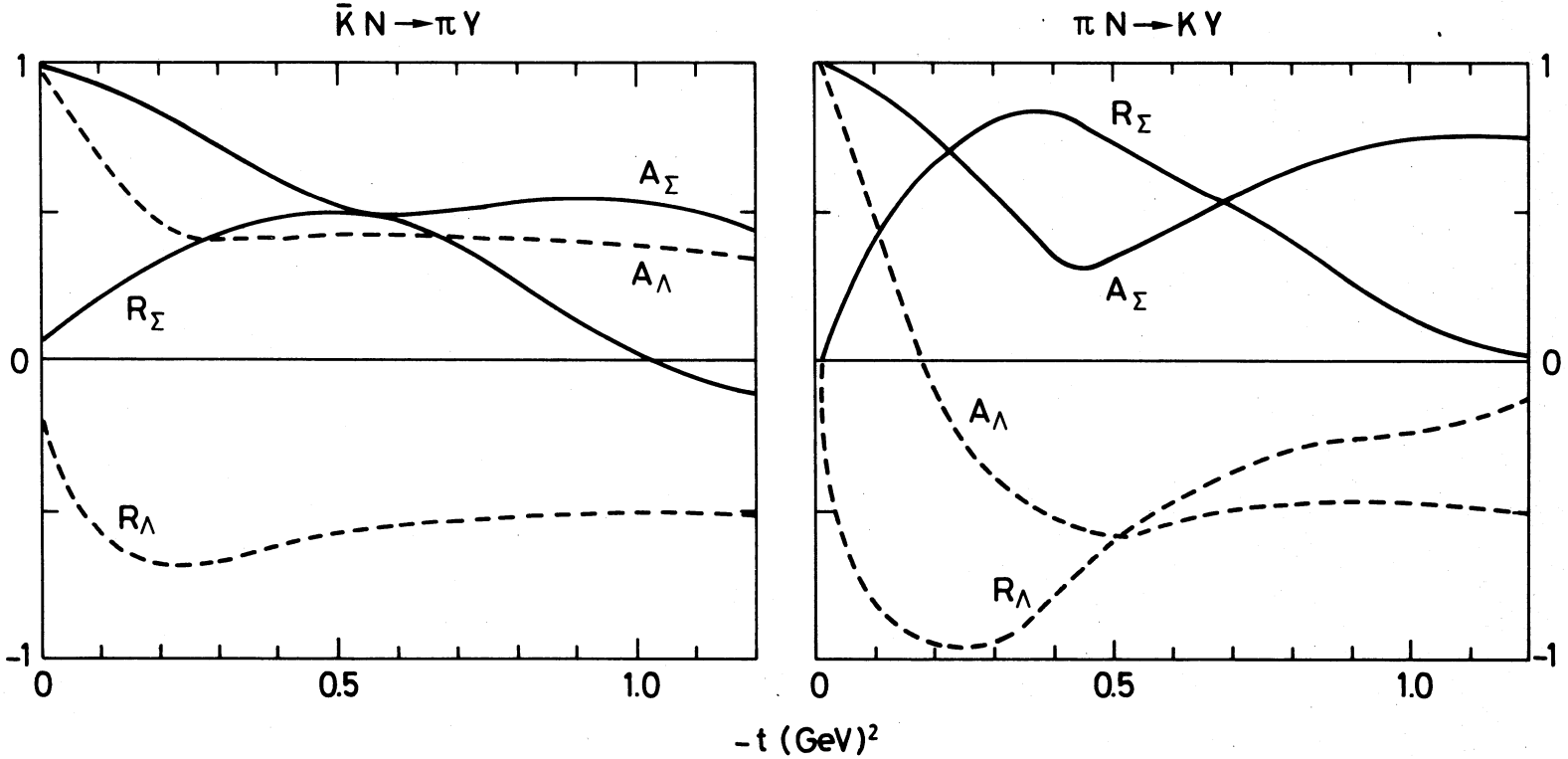

FIG.13